

# Galaxy merging in MOND

Carlo Nipoti<sup>1</sup>, Pasquale Londrillo<sup>2</sup>, and Luca Ciotti<sup>1</sup>

<sup>1</sup>*Astronomy Department, University of Bologna, via Ranzani 1, 40127 Bologna, Italy*

<sup>2</sup>*INAF-Bologna Astronomical Observatory, via Ranzani 1, 40127 Bologna, Italy*

Accepted 2007 August 7. Received 2007 July 25; in original form 2007 May 31

## ABSTRACT

We present the results of N-body simulations of dissipationless galaxy merging in Modified Newtonian Dynamics (MOND). For comparison, we also studied Newtonian merging between galaxies embedded in dark matter halos, with internal dynamics equivalent to the MOND systems. We found that the merging timescales are significantly longer in MOND than in Newtonian gravity with dark matter, suggesting that observational evidence of rapid merging could be difficult to explain in MOND. However, when two galaxies eventually merge, the MOND merging end-product is hardly distinguishable from the final stellar distribution of an equivalent Newtonian merger with dark matter.

**Key words:** gravitation — stellar dynamics — galaxies: kinematics and dynamics

## 1 INTRODUCTION

Given the remarkable ability of MOND to reproduce the kinematics of galaxies (e.g., Milgrom 2002; Sanders & McGaugh 2002) and its increased interest due to the possibility of a relativistic formulation (Bekenstein 2004), it is natural to look for tests able to discriminate between MOND and Newtonian gravity with dark matter (DM). Despite numerous attempts, no clear-cut cases have been found so far (see Bekenstein 2006), the main reason being that MOND is a non-linear theory, and this makes the study of systems deviating significantly from spherical symmetry (Brada & Milgrom 1995; Ciotti, Londrillo & Nipoti 2006) and the performance of N-body simulations more difficult in MOND than in Newtonian dynamics. In particular, very few N-body simulations of MOND systems have been performed so far, exploring stability of disk galaxies (Brada & Milgrom 1999; Tiret & Combes 2007), external field effect (Brada & Milgrom 2000), dissipationless collapse and phase mixing (Nipoti, Londrillo & Ciotti 2007a, hereafter NLC07; Ciotti, Nipoti & Londrillo 2007). In addition, the study of structure formation in MOND using N-body cosmological simulations is still limited to a couple of preliminary explorations (Nusser 2002; Knebe & Gibson 2004).

Observations leave no doubt that galaxy merging occurs (e.g. Arp 1966; Schweizer 1982), and it is also known that Newtonian gravity can account in detail for such a process (Toomre & Toomre 1972). It is then natural to study galaxy merging in MOND. In fact, there are reasons to expect that galaxy merging is less effective in MOND than in Newtonian gravity: in MOND galaxies are expected to collide at high speed, and there are no DM halos to absorb orbital energy and angular momentum (Binney 2004; Sellwood 2004); in

addition, it has been recently shown that violent relaxation and phase mixing are slower in MOND (NLC07; Ciotti et al. 2007).

Taking advantage of our recently developed MOND N-body code, in this Letter we present the results of N-body simulations of galaxy merging in MOND, focusing for simplicity on the case of dissipationless merging between equal-mass spherical galaxies. For comparison, we also consider the merging of structurally identical purely baryonic Newtonian systems, and the merging of equivalent Newtonian systems (i.e., Newtonian models with the same baryonic distribution as the MOND systems, embedded in DM halos such that their internal dynamics matches the corresponding MOND cases; see Milgrom 2001; Nipoti et al. 2007b).

## 2 THE NUMERICAL SIMULATIONS

We consider MOND in Bekenstein & Milgrom’s (1984) formulation, in which the Poisson equation  $\nabla^2\phi^N = 4\pi G\rho$  is substituted by the non-relativistic field equation

$$\nabla \cdot \left[ \mu \left( \frac{\|\nabla\phi\|}{a_0} \right) \nabla\phi \right] = 4\pi G\rho. \quad (1)$$

In the equation above  $\|\dots\|$  is the standard Euclidean norm,  $\phi$  and  $\phi^N$  are, respectively, the MOND and Newtonian gravitational potentials produced by  $\rho$ , and for finite mass systems  $\nabla\phi \rightarrow 0$  for  $\|\mathbf{x}\| \rightarrow \infty$ . The function  $\mu(y)$  is not constrained by the theory except that it must run smoothly from  $\mu(y) \sim y$  at  $y \ll 1$  (in the so-called deep-MOND regime) to  $\mu(y) \sim 1$  at  $y \gg 1$ , with a dividing acceleration scale  $a_0 \simeq 1.2 \times 10^{-10} \text{ m s}^{-2}$ , and in the present work we adopt  $\mu(y) = y/\sqrt{1+y^2}$  (Milgrom 1983). From the Pois-

**Table 1.** Parameters of the simulations and properties of the end-products.

Name (1)	Gravity (2)	$M_{\text{DM}}/M_*$ (3)	$\kappa$ (4)	$v_0/v_*$ (5)	$b_0/d_0$ (6)	$N_*$ (7)	$N_{\text{DM}}$ (8)	$c/a$ (9)	$b/a$ (10)	$r_{\text{M}}/r_{\text{M},0}$ (11)	$\sigma_{\text{V}}/\sigma_{\text{V},0}$ (12)	$\gamma$ (13)	$\langle m \rangle$ (14)
M1h	MOND	0	1	0.958	0	$2 \times 10^6$	0	0.52	0.54	1.6	1.09	$1.4 \pm 0.3$	$4.4 \pm 0.3$
E1h	Newton	30	1	1.017	0	$2 \times 10^5$	$2 \times 10^6$	0.48	0.50	1.2	1.22	$1.0 \pm 0.2$	$3.4 \pm 0.3$
M1o	MOND	0	1	0.958	0.5	$2 \times 10^6$	0	0.51	0.61	1.9	1.09	$2.0 \pm 0.3$	$6.3 \pm 0.3$
E1o	Newton	30	1	1.017	0.5	$2 \times 10^5$	$2 \times 10^6$	0.54	0.60	1.2	1.23	$1.3 \pm 0.2$	$4.1 \pm 0.2$
M25h	MOND	0	25	0.428	0	$2 \times 10^6$	0	0.54	0.73	2.1	1.16	$1.8 \pm 0.3$	$4.2 \pm 0.3$
E25h	Newton	5	25	0.447	0	$2 \times 10^5$	$1 \times 10^6$	0.52	0.57	1.5	1.27	$1.3 \pm 0.3$	$3.5 \pm 0.3$
M25o	MOND	0	25	0.428	0.5	$2 \times 10^6$	0	0.59	0.79	2.2	1.16	$2.0 \pm 0.3$	$6.3 \pm 0.5$
E25o	Newton	5	25	0.447	0.5	$2 \times 10^5$	$1 \times 10^6$	0.62	0.83	1.3	1.29	$1.7 \pm 0.3$	$4.5 \pm 0.3$
N0h	Newton	0	-	0.183	0	$2 \times 10^6$	0	0.68	0.71	2.0	1.07	$2.0 \pm 0.1$	$5.0 \pm 0.3$
N0o	Newton	0	-	0.183	0.5	$2 \times 10^6$	0	0.64	0.89	1.6	1.07	$2.1 \pm 0.2$	$5.5 \pm 0.3$

(1): name of the simulation. (2): gravity law. (3): DM to baryonic mass ratio. (4): internal acceleration ratio. (5): normalised relative speed of the barycentres at  $t = 0$ . (6): normalised impact parameter at  $t = 0$  (in all cases  $d_0 = 40r_*$ ). (7): total number of stellar particles. (8): total number of DM particles. (9): end-product minor-to-major axis ratio. (10): end-product intermediate-to-major axis ratios. (11): final-to-initial half-mass radius ratio. (12): final-to-initial virial velocity dispersion ratio. (13): best-fit inner logarithmic slope of the final angle-averaged density profile. (14): best-fit Sersic index of the final projected density profile.

son equation and equation (1) it follows that the MOND ( $\mathbf{g} = -\nabla\phi$ ) and Newtonian ( $\mathbf{g}^{\text{N}} = -\nabla\phi^{\text{N}}$ ) gravitational fields are related by  $\mu(g/a_0)\mathbf{g} = \mathbf{g}^{\text{N}} + \mathbf{S}$ , where  $g \equiv \|\mathbf{g}\|$ , and  $\mathbf{S}$  is a solenoidal field dependent on the specific  $\rho$  considered: in general one cannot impose  $\mathbf{S} = 0$ , thus the use of standard Poisson solvers to develop MOND N-body codes is not possible, and equation (1) must be solved at each time step (Brada & Milgrom 1999; NLC07).

## 2.1 Initial conditions and the code

The baryonic component of the initial conditions of all the simulations presented in this paper consists of two identical galaxy models with stellar density distribution

$$\rho_*(r) = \frac{M_*}{2\pi} \frac{r_*}{r(r+r_*)^3}, \quad (2)$$

where  $M_*$  is the total stellar mass and  $r_*$  is the core radius (Hernquist 1990). To each MOND model with potential  $\phi$  corresponds an *equivalent* Newtonian model with  $\phi^{\text{N}} = \phi$ , thus having a DM halo with density  $\rho_{\text{DM}}(r) = \nabla^2\phi(r)/4\pi G - \rho_*(r)$ . In principle, such a DM halo would have infinite mass, so we truncate it at  $r \sim 30r_*$ . For completeness, we also ran simulations of Newtonian merging between purely baryonic systems with the same stellar density distribution (2) and no DM halo.

The particles of the stellar component are distributed with the standard rejection technique applied to the phase-space distribution function (DF), restricting for simplicity to the fully isotropic case. In the purely baryonic Newtonian case the DF is known explicitly (Hernquist 1990), while in MOND the corresponding DF is obtained numerically with an Eddington inversion (e.g. Binney & Tremaine 1987)

$$f_{\text{M}}(E) = \frac{1}{\sqrt{8\pi^2}} \frac{d}{dE} \int_E^\infty \frac{d\rho_*}{d\phi} \frac{d\phi}{\sqrt{\phi - E}}, \quad (3)$$

where the upper integration limit reflects the far-field logarithmic behaviour of the MOND potential (see also Angus, Famaey & Zhao 2006). Finally, in the equivalent Newtonian models the stellar particles are distributed by using

their numerical two-component isotropic DF. However, this is not possible in general for the equivalent DM halo particles, because for systems with sufficiently high stellar surface density the resulting halo presents a central hole, and so it cannot be derived from an everywhere positive, isotropic DF<sup>1</sup> (Ciotti & Pellegrini 1992). Thus, the initial DM particle velocities are extracted from a Maxwellian distribution with local velocity dispersion satisfying the isotropic two-component Jeans' equations. We verified that the resulting models are in approximate equilibrium by evolving them in isolation for several dynamical times.

We consider both head-on and off-centre encounters. In the head-on cases (impact parameter  $b_0 = 0$ ) the two galaxies are released at  $t = 0$  with barycentric distance  $d_0 = 40r_*$ , and with the relative speed  $v_0$  that they would have if they started at rest at  $d_{\text{rest}} = 60r_*$ . Thus, in the Newtonian cases

$$v_0^2 = 4G(M_* + M_{\text{DM}}) \left( \frac{1}{d_0} - \frac{1}{d_{\text{rest}}} \right), \quad (4)$$

while in the MOND cases

$$v_0^2 \simeq 0.8\sqrt{8GM_*a_0} \ln \frac{d_{\text{rest}}}{d_0}, \quad (5)$$

where we have used the approximate expression of the force between two particles in deep-MOND regime (Milgrom 1986; Milgrom 1994). In the off-centre cases,  $d_0$  and  $v_0$  are the same as in the corresponding head-on cases, but the relative velocity is oriented so that the impact parameter  $b_0 = d_0/2$ .

The physical scales of the problem are introduced as follows. First of all, we identify each MOND initial condition by fixing a value for the dimensionless internal acceleration parameter  $\kappa \equiv GM_*/(a_0r_*^2)$ , so  $M_*$  and  $r_*$  are not independent quantities: in physical units,  $r_* \simeq 3.4\kappa^{-1/2}M_{*,10}^{1/2}$  kpc, where  $M_{*,10} \equiv M_*/10^{10}M_\odot$ . The time and velocity units are  $t_* = \sqrt{r_*^3/GM_*} \simeq 29.7\kappa^{-3/4}M_{*,10}^{1/4}$  Myr, and  $v_* = r_*/t_* \simeq$

<sup>1</sup> This result shows that it is important to check the positivity of the DF (and not only that of  $\rho_{\text{DM}}$ ), when studying Newtonian systems with DM equivalent to MOND models.

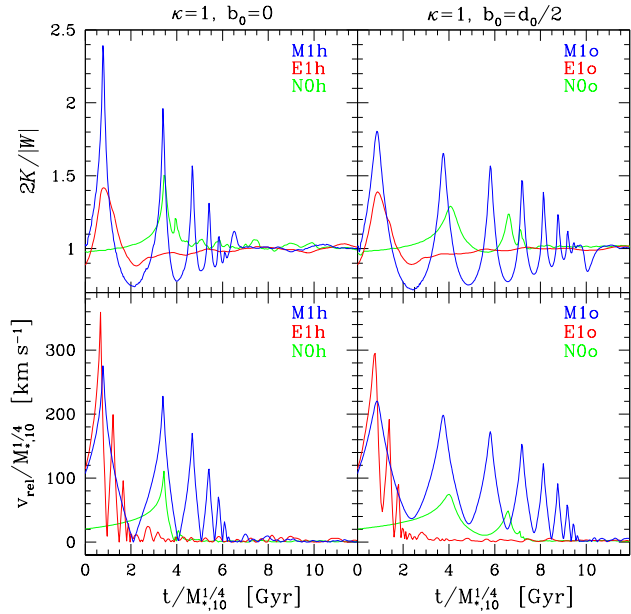


**Figure 1.** Time evolution of the virial ratio (top panels) and of the barycentric relative speed (bottom panels) for the two sets of simulations with  $\kappa = 1$ : head-on (left panels) and off-centre (right panels). Blue, red, and green curves refer to MOND, equivalent Newtonian, and purely baryonic Newtonian simulations, respectively. For the scaling of time and velocity, see Section 2.1.

$112\kappa^{1/4}M_{*,10}^{1/4}\text{ km s}^{-1}$  (see NLC07 for a more detailed discussion of the normalisations). The simulations are evolved up to  $t = 400t_*$  ( $\kappa = 1$  cases) or  $t = 500t_*$  ( $\kappa = 25$  and purely baryonic Newtonian cases), which amount to several gigayears in physical units for galaxy masses in the observed range.

Our MOND N-body code (NLC07) is a parallel three-dimensional particle-mesh code that can be used to run MOND as well as Newtonian simulations. The code is based on a grid in spherical coordinates, on which the MOND potential is computed by solving exactly the field equation (1) with the iterative potential solver (based on spectral methods) described in Ciotti et al. (2006). Particle-mesh interpolations are obtained with a quadratic spline in each coordinate, while time stepping is given by a classical leap-frog scheme. The time step is the same for all particles and is allowed to vary adaptively in time. Given the spherical geometry of the grid, the code is not best-suited to run merging simulations: in order to obviate this difficulty, we used a time-adaptive grid with a much larger number of grid points ( $128^3$ ) than in the collapse simulations of NLC07. With this resolution, we obtained excellent agreement between Newtonian merging simulations run with the MOND code and simulations (starting from the same initial conditions) run with our FVFPS treecode (Fortran Version of a Fast Poisson Solver; Londrillo, Nipoti & Ciotti 2003; Nipoti, Londrillo & Ciotti 2003). In summary, all the presented simulations were run with the MOND code, and the Newtonian simulations also with the FVFPS code. The properties of the simulations, including the total number of stellar ( $N_*$ ) and DM ( $N_{\text{DM}}$ ) particles used, are summarised in Table 1.

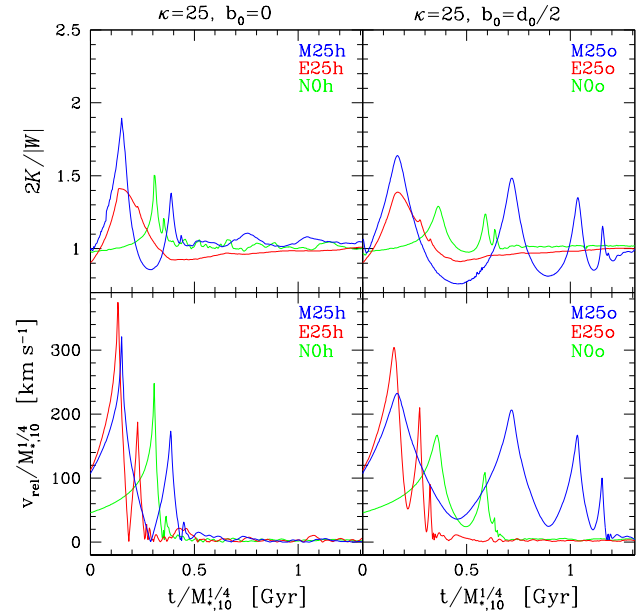


**Figure 2.** The same as Fig. 1, but for the two sets of simulations with  $\kappa = 25$ : head-on (left panels) and off-centre (right panels).

## 3 RESULTS

### 3.1 Merging dynamics and timescales

We present now the results of four sets of merging simulations, each characterised by a combination of the value of the internal acceleration parameter ( $\kappa = 1$  or  $\kappa = 25$ ) and of the impact parameter ( $b_0 = 0$  or  $b_0 = d_0/2$ ). Each set comprises three simulations: MOND, equivalent Newtonian ( $M_{\text{DM}} = 30M_*$  for  $\kappa = 1$ , and  $M_{\text{DM}} = 5M_*$  for  $\kappa = 25$ ) and purely baryonic Newtonian. In the top panels of Figs. 1 and 2 we show the time evolution of the virial ratio  $2K/|W|$  (where  $K$  is the total kinetic energy and  $W$  is the trace of the Chandrasekhar potential energy tensor) and, in the bottom panels, the time evolution of the relative speed  $v_{\text{rel}}$  of the barycentres of the two galaxies: note that the time and velocity units are the same for all simulations. Peaks in  $2K/|W|$  and in  $v_{\text{rel}}$  correspond to close encounters between the two systems, while minima of  $2K/|W|$  and  $v_{\text{rel}}$  occur when the separation is maximum. At the end of all the presented simulations  $2K/|W| \sim 1$  and  $v_{\text{rel}} \sim 0$ , indicating that the two systems merged, forming a single virialised object.

Let us focus first on the case  $\kappa = 1$ , in which the initial galaxies, having internal accelerations everywhere lower than  $a_0$ , are in deep-MOND regime. As can be seen from Fig. 1, in both the head-on and the off-centre cases, the merging timescale is apparently longer in MOND (blue curves) than in the equivalent Newtonian simulations (red curves). In MOND the two galaxies experience several close encounters before merging, while in the equivalent Newtonian cases they merge quickly after the first close passage. The behaviour of both MOND and purely baryonic Newtonian cases (green curves) is very sensitive to whether the orbit is head-on or off-centre: the merging timescale in simulation N0o is almost a factor of two longer than in simulation N0h, and also simulation M1o takes significantly longer to virialise than simulation M1h. In contrast, due to the

presence of DM halos, the merging timescale is as short in the off-centre as in head-on the equivalent Newtonian cases. As expected, the relative speed during the first close encounter is significantly higher in MOND simulations than in the purely baryonic ones. On the other hand, the equivalent Newtonian models collide at higher speed than their MOND counterparts. We note that this last result depends on the specific choice of  $M_{\text{DM}}$  and  $d_{\text{rest}}$  appearing in equations (4) and (5): provided that  $d_0$  is large enough MOND would have no problem in attaining arbitrarily high collision speeds (see also Angus & McGaugh 2007 for a discussion of the collision speed of galaxy clusters in MOND).

The case  $\kappa = 25$  (Fig. 2), in which the initial galaxy models have internal accelerations  $\gtrsim a_0$  for  $r \lesssim 5r_*$ , confirms the same trend as the  $\kappa = 1$  case, with merging taking longer in MOND than in equivalent Newtonian models (by a factor of  $\sim 2$  in the head-on case, and by a factor of  $\sim 4$  in the off-centre case). The  $\kappa = 25$  simulations are interesting also because they show how the merging process in MOND is very different from that of purely baryonic Newtonian merging, even when the MOND galaxies are internally in Newtonian regime. This can be easily seen in the head-on simulation M25h, in which the dynamics is almost Newtonian when the two galaxies interpenetrate, but the collision speed is higher than in the purely baryonic Newtonian case, being determined by the long-range deep-MOND interaction between the two galaxies.

We note that the value of  $\kappa$  contains information only on how the *initial* internal accelerations compare with  $a_0$ . A model initially characterised by accelerations everywhere weaker than  $a_0$  can produce accelerations significantly stronger than  $a_0$  during its dynamical evolution. This behaviour was observed by NLC07 in MOND dissipationless collapse simulations (see also Nusser & Pointecouteau 2006, who studied spherically symmetric MOND gaseous collapses in a cosmological context). However, this is not necessarily the case in MOND merging, because during the dissipationless merging process the density does not increase as much as in a collapse. To quantify this effect we computed at each time step the fraction of particles with acceleration stronger than  $a_0$ . In simulations M25h and M25o this fraction is initially  $\sim 0.3$ , has a peak up to  $\sim 0.5$  during the first close passage, and is again  $\sim 0.3$  in the end-products. On the other hand, it turns out that in simulations M1h and M1o this fraction is  $\lesssim 0.02$  throughout the entire simulation: in other words our  $\kappa = 1$  simulations are in deep-MOND regime at all times.

From an observational point of view, simulations with  $\kappa = 1$  can represent merging between two dwarf spheroidal galaxies with  $M_* = 10^7 M_\odot$  (and effective radius  $R_e \sim 0.2$  kpc, so the merging timescale would be  $\lesssim 1.8$  Gyr), while simulations with  $\kappa = 25$  can represent merging between two luminous elliptical galaxies with  $M_* \sim 10^{11} M_\odot$  (and effective radius  $R_e \sim 4$  kpc, so the merging timescale would be  $\lesssim 2.1$  Gyr). Thus, restricting to the presented cases, one could be tempted to conclude that galaxies in MOND can merge in a timescale significantly shorter than the Hubble time. However, we stress that such a conclusion is wrong in a general sense, because we reported only cases with orbital energies corresponding to two galaxies at rest when at relatively small distance ( $d_{\text{rest}} \simeq 25r_{\text{M},0}$ , where  $r_{\text{M},0}$  is the half-mass radius of the initial stellar distributions). Given

the logarithmic nature of the MOND gravitational potential (see equation 5), choosing larger values of  $d_{\text{rest}}$  has the effect of boosting the encounter relative speed (making the merging process difficult), while it barely affects the encounter speed in Newtonian gravity. In fact, we explored several other cases of MOND encounters, with larger  $d_{\text{rest}}$  (and then higher  $v_0$ ), but we had to stop the simulations, because the two galaxies after the first close passage reach relative distances significantly larger than  $d_0$ , making the required computational time exceedingly long, revealing virialisation times even longer than the age of the Universe (note that the MOND simulation in the right panels of Fig. 1 is already dangerously long). Summarising, we presented here only simulations of encounters relatively favourable to merging in MOND, and yet these mergings were found to be less effective than in Newtonian gravity with DM.

### 3.2 Merging end-products

We define merging end-products the systems comprising the bound *stellar* particles at the end of the simulation. In the Newtonian simulations we found that  $\lesssim 4$  per cent of the stellar particles escaped, while there cannot be escapers in the MOND cases. Using the same procedure as in NLC07, we determined the following properties of the end-products: the axis ratios  $c/a$  and  $b/a$  of the inertia ellipsoid, the angle-averaged half-mass radius  $r_{\text{M}}$ , the virial velocity dispersion  $\sigma_{\text{V}}$ , the inner slope  $\gamma$  of the  $\gamma$ -model (Dehnen 1993; Tremaine et al. 1994) that best fits the final angle-averaged density profile (over the radial range  $0.1 \lesssim r/r_{\text{M}} \lesssim 10$ ), and, for the three principal axis projections, the circularised effective radius  $R_e$  and the index  $m$  of the Sersic (1968) law that best fits the circularised projected density profile over the radial range  $0.1 \lesssim R/R_e \lesssim 10$  (see Table 1, where  $\langle m \rangle$  is the average of the values of  $m$  obtained for the three projections).

The structural and kinematic properties of the MOND end-products are not significantly different from those of their Newtonian equivalent counterparts: for instance, the final axis ratios are roughly the same in corresponding MOND and equivalent Newtonian simulations (see Table 1). The end-products of simulations E1h and E1o are DM dominated at all radii, and similarly the end-products of the  $\kappa = 1$  MOND mergers are everywhere in deep-MOND regime (so they would appear as DM dominated at all radii if interpreted in Newtonian gravity). On the other hand, the  $\kappa = 25$  MOND end-products would appear in Newtonian gravity as baryon-dominated in the inner regions ( $r/r_{\text{M}} \lesssim 1.2 - 1.3$ ) and DM dominated at larger radii; the corresponding equivalent Newtonian end-products are baryon dominated at radii  $r/r_{\text{M}} \lesssim 0.4 - 0.5$ . In general both MOND and equivalent end-products have rather flat intrinsic and projected velocity dispersion profiles. The MOND final density profiles tend to be steeper ( $\gamma = 1.4 - 2.0$ ,  $\langle m \rangle = 4.2 - 6.3$ ) than those of the equivalent Newtonian cases ( $\gamma = 1.0 - 1.7$ ,  $\langle m \rangle = 3.4 - 4.5$ ), but there is not a dichotomy between the two families.

An interesting point (in the context of the galaxy scaling relations) is how the final virial velocity dispersion  $\sigma_{\text{V}}$  and half-mass radius  $r_{\text{M}}$  compare with the corresponding quantities in the initial systems  $\sigma_{\text{V},0}$  and  $r_{\text{M},0}$  (Nipoti et al. 2003). MOND mergers have larger  $r_{\text{M}}$  and lower  $\sigma_{\text{V}}$  than the corresponding equivalent Newtonian mergers. We also note that in the Newtonian cases here presented the ratio

$\sigma_V/\sigma_{V,0}$  tend to be larger (and  $r_M/r_{M,0}$  smaller) than in similar cases explored in Nipoti et al. (2003): this is expected, because here we consider elliptic orbits while Nipoti et al. (2003) considered parabolic orbits.

#### 4 DISCUSSION AND CONCLUSIONS

The main result of the present work is that galaxy merging is much less effective in MOND than in Newtonian dynamics with DM. In addition, the derived MOND merging timescales must be considered only lower limits, because rather specific orbital properties are required in MOND in order to have galaxy mergers on timescales shorter than the age of the Universe. In general, repeated high speed galaxy encounters should be a common feature of galaxy interactions in MOND, while any observational evidence of rapid merging after the first close passage should be regarded as an indication of the presence of DM halos. Remarkably, when the orbital parameters are favourable and two galaxies eventually merge in MOND, the merging end-product is hardly distinguishable from the final stellar distribution of an equivalent Newtonian merger with DM.

Thus, the very observation of galaxy mergers appears to favour the DM scenario with respect to the MOND hypothesis. Additional constraints for galaxy merging in MOND could be also given by specific dynamical features in galaxy interactions that have extensively studied and explained in the context of Newtonian gravity (e.g. Binney & Tremaine 1987), such as the tidal tails observed around interacting disk galaxies as the “Antennae” pair of galaxies NGC 4038/NGC 4039 (Toomre & Toomre 1972), and the surface brightness ripples observed in the outskirts of luminous elliptical galaxies as NGC 3923 (Quinn 1984).

The result that merging is less effective in MOND than in a DM scenario appears consistent with our previous findings that phase-mixing and violent relaxation are slower in MOND than in Newtonian gravity (NLC07; Ciotti et al. 2007). The merging process is intimately related also to dynamical friction, so our simulations might be interpreted as an indication that dynamical friction is less effective in MOND than in Newtonian gravity with DM, in contrast with the analytical estimates of Ciotti & Binney (2004) for the case of a particle moving in a homogeneous medium. However, the complexity of the merging process prevents us from drawing firm conclusions on this issue, and we plan to realise ad hoc numerical experiments to explore in detail dynamical friction in MOND.

We must also recall that we explored only very simple cases of galaxy merging in MOND: in particular, we only considered equal-mass dissipationless merging between spherical systems, while dissipative processes in the merging of gas-rich galaxies might be effective in making the merging timescales shorter. Another possible caveat is that, given the long-range nature of MOND gravity, the restriction to an isolated pair of galaxies might not be as justified as in Newtonian gravity, and the next step to address this point would be the study of galaxy merging in MOND in a cosmological context. A valuable contribution in this direction would be the performance of cosmological simulations of structure formation, based on a self-consistent relativistic formulation of MOND such as Bekenstein’s (2004) TeVeS.

#### ACKNOWLEDGEMENTS

We are grateful to James Binney and Alar Toomre for helpful discussions. We also thank the anonymous Referee for useful comments on the manuscript. Some of the numerical simulations were performed using the CLX system at CINECA, Bologna, with CPU time assigned under the INAF-CINECA agreement 2006/2007.

#### REFERENCES

- Angus G.W., McGaugh S.S., 2007, preprint (arXiv:0704.0381v1)  
 Angus G.W., Famaey B., Zhao H.S., 2006, MNRAS, 371, 138  
 Arp H., 1966, Atlas of Peculiar Galaxies, Carnegie Institution, Washington D.C.  
 Bekenstein J., 2004, Phys. Rev. D, 70, 3509  
 Bekenstein J., 2006, Contemporary Physics, 47, 387  
 Bekenstein J., Milgrom M., 1984, ApJ, 286, 7  
 Binney J., 2004, in Ryder S.D., Pisano D.J., Walker M.A., Freeman K.C., eds, IAU Symp. 220, Dark Matter in Galaxies. Astron. Soc. Pac., San Francisco, p. 3  
 Binney J., Tremaine S., 1987, Galactic Dynamics, Princeton University Press, Princeton  
 Brada R., Milgrom M., 1995, MNRAS, 276, 453  
 Brada R., Milgrom M., 1999, ApJ, 519, 590  
 Brada R., Milgrom M., 2000, ApJ, 541, 556  
 Ciotti L., Binney J., 2004, MNRAS, 351, 285  
 Ciotti L., Pellegrini S., 1992, MNRAS, 255, 561  
 Ciotti L., Londrillo P., Nipoti C., 2006, ApJ, 640, 741  
 Ciotti L., Nipoti C., Londrillo P., 2007, in Collective Phenomena in Macroscopic Systems, ed. G. Bertin et al. (Singapore: World Scientific), in press (arXiv:astro-ph/0701826v1)  
 Dehnen W., 1993, MNRAS, 265, 250  
 Hernquist L., 1990, ApJ, 356, 359  
 Knebe A., Gibson B.K., 2004, MNRAS, 347, 1055  
 Londrillo P., Nipoti C., Ciotti L., 2003, In “Computational astrophysics in Italy: methods and tools”, Roberto Capuzzo-Dolcetta ed., Mem. S.A.It. Supplement, vol. 1, p. 18  
 Milgrom M., 1983, ApJ, 270, 365  
 Milgrom M., 1986, ApJ, 302, 617  
 Milgrom M., 1994, ApJ, 429, 540  
 Milgrom M., 2001, MNRAS, 326, 1261  
 Milgrom M., 2002, New. Astron. Rev., 46, 741  
 Nipoti C., Londrillo P., Ciotti L., 2003, MNRAS, 342, 501  
 Nipoti C., Londrillo P., Ciotti L., 2007a, ApJ, 660, 256 (NLC07)  
 Nipoti C., Londrillo P., Zhao H.S., Ciotti L., 2007b, MNRAS in press (arXiv:0704.0740v2)  
 Nusser A., 2002, MNRAS, 331, 909  
 Nusser A., Pointecouteau E., 2006, MNRAS, 366, 96  
 Quinn P.J., 1984, ApJ, 279, 596  
 Sanders R., McGaugh S., 2002, ARA&A, 40, 263,  
 Schweizer F., 1982, ApJ, 252, 455  
 Sellwood J., 2004, in Ryder S.D., Pisano D.J., Walker M.A., Freeman K.C., eds, IAU Symp. 220, Dark Matter in Galaxies. Astron. Soc. Pac., San Francisco, p. 27  
 Sersic J.L., 1968, Atlas de galaxias australes. Observatorio Astronomico, Cordoba  
 Tiret O., Combes F., 2007, A&A, 464, 517  
 Toomre A., Toomre J., 1972, ApJ, 178, 623  
 Tremaine S., Richstone D.O., Yong-Ik B., Dressler A., Faber S.M., Grillmair C., Kormendy J., Lauer T.R., 1994, AJ, 107, 634